

Multielectron C–O Bond Activation Mediated by a Family of Reduced Uranium Complexes

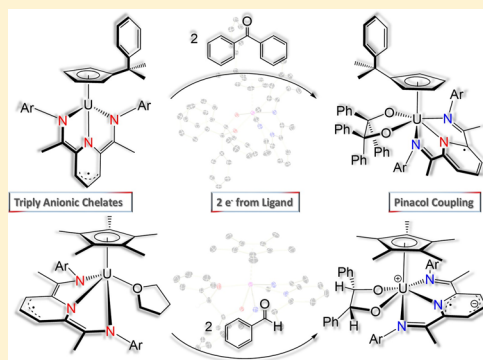
John J. Kiernicki,[†] Brian S. Newell,[‡] Ellen M. Matson,[†] Nickolas H. Anderson,[†] Phillip E. Fanwick,[†] Matthew P. Shores,[‡] and Suzanne C. Bart^{*,†}

[†]H.C. Brown Laboratory, Department of Chemistry, Purdue University, West Lafayette, Indiana 47906, United States

[‡]Department of Chemistry, Colorado State University, Fort Collins, Colorado 80523, United States

Supporting Information

ABSTRACT: A family of cyclopentadienyl uranium complexes supported by the redox-active pyridine(diimine) ligand, $^{\text{Mes}}\text{PDI}^{\text{Me}}$ ($^{\text{Mes}}\text{PDI}^{\text{Me}} = 2,6-((\text{Mes})\text{N}=\text{CMe})_2\text{-C}_5\text{H}_3\text{N}$, Mes = 2,4,6-trimethylphenyl), has been synthesized. Using either Cp^* or Cp^{P} ($\text{Cp}^* = 1,2,3,4,5\text{-pentamethylcyclopentadienide}$, $\text{Cp}^{\text{P}} = 1\text{-}(7,7\text{-dimethylbenzyl})\text{cyclopentadienide}$), uranium complexes of the type $\text{Cp}^{\text{X}}\text{U}(\text{MesPDI}^{\text{Me}})_2$ (**1-Cp^X**; X = * or P), $\text{Cp}^{\text{X}}\text{UI}(\text{MesPDI}^{\text{Me}})$ (**2-Cp^X**), and $\text{Cp}^{\text{X}}\text{U}(\text{MesPDI}^{\text{Me}})(\text{THF})_n$ (**3-Cp^X**; *, $n = 1$; P, $n = 0$) were isolated and characterized. The series was generated via ligand centered reduction events; thus the extent of $^{\text{Mes}}\text{PDI}^{\text{Me}}$ reduction varies in each case, but the uranium(IV) oxidation state is maintained. Treating **2-Cp^X**, which has a doubly reduced $^{\text{Mes}}\text{PDI}^{\text{Me}}$, with furfural results in radical coupling between the substrate and $^{\text{Mes}}\text{PDI}^{\text{Me}}$, leading to C–C bond formation to form $\text{Cp}^{\text{X}}\text{UI}(\text{MesPDI}^{\text{Me}}\text{-CHOC}_4\text{H}_3\text{O})$ (**4-Cp^X**). Exposure of **3-Cp^{*}** and **3-Cp^P**, which contain a triply reduced $^{\text{Mes}}\text{PDI}^{\text{Me}}$ ligand, to benzaldehyde and benzophenone, respectively, results in the corresponding pinacolate complexes $\text{Cp}^*\text{U}(\text{O}_2\text{C}_2\text{Ph}_2\text{H}_2)(^{\text{Mes}}\text{PDI}^{\text{Me}})$ (**5-Cp^{*}**) and $\text{Cp}^{\text{P}}\text{U}(\text{O}_2\text{C}_2\text{Ph}_4)(^{\text{Mes}}\text{PDI}^{\text{Me}})$ (**5-Cp^P**). The reducing equivalents required for this coupling are derived solely from the redox-active ligand, rather than the uranium center. Complexes **1–5** have been characterized by ^1H NMR and electronic absorption spectroscopies, and SQUID magnetometry was employed to confirm the mono(anionic) [$^{\text{Mes}}\text{PDI}^{\text{Me}}$] $^-$ ligand in **1-Cp^P** and **5-Cp^P**. Structural parameters of complexes **1-Cp^P**, **2-Cp^X**, **4-Cp^{*}**, and **5-Cp^X** have been elucidated by X-ray crystallography.



INTRODUCTION

Among the first organouranium complexes reported were those bearing cyclopentadienyl ligands, including Cp_3U ,^{1,2} Cp_3UCl ,¹ and Cp_4U .³ Since that time, the field of organoactinide chemistry has been dominated by variations of these frameworks, with a particular emphasis on the bulky permethylated derivative, 1,2,3,4,5-pentamethylcyclopentadienide (Cp^*).^{4–12} The bis(Cp^*) metallocene framework supports uranium compounds in varying oxidation states^{13–17} and provides steric protection to eliminate unwanted side reactions while focusing desired reactivity at the metallocene wedge.

By comparison, significantly fewer studies focus on the piano stool variation for uranium compounds. Using a single Cp ring provides the desired steric protection at one face of uranium, while facilitating easy steric and electronic tuning at vacant coordination sites by introducing non-Cp-based ligands. Because cyclopentadienyl ligands offer little in the way of redox flexibility, incorporation of redox-active ligands at these positions can promote multielectron chemistry in addition to easier tunability. This was recently demonstrated by Evans with the synthesis of the family of Cp^* uranium dimers that feature a bridging, two-electron reduced benzene ring, $[\text{Cp}^*(\text{Y})\text{U}]_2(\mu\text{-}\eta^6\text{:}\eta^6\text{-C}_6\text{H}_6)$ (Y = $-\text{OAr}$ (OAr = 2,6-bis(*tert*-butyl)-4-

methylphenolate), $-\text{CH}(\text{SiMe}_3)_2$, $-\text{N}(\text{SiMe}_3)_2$, $^i\text{PrNC}(\text{Me})\text{-N}^i\text{Pr}$).¹⁸ These complexes act as four electron reductants toward small molecules, such as cyclooctatetraene or azidoadamantane, forming the corresponding uranium(VI) products.

Recently, we adapted this strategy with the report of the synthesis and characterization of $\text{Cp}^*\text{U}(\text{MesPDI}^{\text{Me}})(\text{THF})$ (**3-Cp^{*}**), which has a trianionic [$^{\text{Mes}}\text{PDI}^{\text{Me}}$] $^{3-}$ ligand.¹⁹ The three reducing equivalents stored in the pyridine(diimine) ligand, plus one from uranium, can be used for the four-electron N=N double bond cleavage of azobenzene to produce the uranium(V) bis(imido) $\text{Cp}^*\text{U}(\text{MesPDI}^{\text{Me}})(\text{NPh})_2$, which has a neutral [$^{\text{Mes}}\text{PDI}^{\text{Me}}$] 0 . On the basis of the success of **3-Cp^{*}** for bond activation reactions, additional reduced species were targeted to determine if a family with differing steric and electronic properties of the Cp ring could be generated. Herein, we report the sequential reduction of two series of uranium complexes bearing cyclopentadienyl ancillary ligands and a redox-active pyridine(diimine). Exposure of these species to

Received: January 7, 2014

Published: March 10, 2014

both aldehydes and ketones results in either ligand or pinacol radical coupling from ligand-based oxidation events.

EXPERIMENTAL SECTION

General Considerations. All air- and moisture-sensitive manipulations were performed using standard Schlenk techniques or in an MBraun inert atmosphere drybox with an atmosphere of purified nitrogen. The MBraun drybox was equipped with a cold well designed for freezing samples in liquid nitrogen as well as two $-35\text{ }^{\circ}\text{C}$ freezers for cooling samples and crystallizations. Solvents for sensitive manipulations were dried and deoxygenated using literature procedures with a Seca solvent purification system.²⁰ Benzene- d_6 was purchased from Cambridge Isotope Laboratories, dried with molecular sieves and sodium, and degassed in three freeze–pump–thaw cycles. A 1.0 M solution of sodium triethylborohydride in toluene was purchased from Sigma-Aldrich and used as received. Benzophenone was purchased from Sigma-Aldrich and recrystallized from dry diethyl ether prior to use. Benzaldehyde and furfural were purchased from Sigma-Aldrich and distilled from magnesium sulfate prior to use. $\text{Cp}^*\text{U}(\text{MesPDI}^{\text{Me}})(\text{THF})_3$ (**3-Cp***),¹⁹ KC_8 ,²¹ $\text{Cp}^*\text{UI}_2(\text{THF})_3$,²² potassium 1-(7,7-dimethylbenzyl)cyclopentadienide (KCp^{P}),²³ $\text{UI}_3(\text{THF})_4$,²⁴ and $\text{MesPDI}^{\text{Me}}$ ($\text{MesPDI}^{\text{Me}} = 2,6\text{-}((\text{Mes})\text{N}=\text{CMe})_2\text{-C}_3\text{H}_3\text{N}$)²⁵ were prepared according to literature procedures.

^1H NMR spectra were recorded on a Varian Inova 300 spectrometer operating at 299.992 MHz. All chemical shifts are reported relative to the peak for SiMe_4 , using ^1H (residual) chemical shifts of the solvent as a secondary standard. The spectra for paramagnetic molecules were obtained by using an acquisition time of 0.5 s; thus the peak widths reported have an error of ± 2 Hz. For paramagnetic molecules, the ^1H NMR data are reported with the chemical shift, followed by the peak width at half height in hertz, the integration value, and, where possible, the peak assignment. Elemental analyses were performed by Midwest Microlab, LLC, Indianapolis, Indiana ($\text{Cp}^{\text{P}}_3\text{U}$, $\text{Cp}^{\text{P}}\text{UI}_2(\text{THF})_3$, **1-Cp^P**, **5-Cp^P**) and Complete Analysis Laboratories, Inc., Parsippany, New Jersey (**2-Cp^P**, **3-Cp^P**, **1-Cp***, **2-Cp***, **4-Cp^P**, **4-Cp***, **5-Cp***). Electronic absorption spectroscopic measurements were recorded at 294 K in sealed 1 cm quartz cuvettes with a Jasco V-6700 spectrophotometer.

Single crystals of **2-Cp*** suitable for X-ray diffraction were coated with poly(isobutylene) oil in a glovebox and quickly transferred to the goniometer head of a Nonius KappaCCD image plate diffractometer equipped with a graphite crystal, incident beam monochromator. Preliminary examination and data collection were performed with Mo $K\alpha$ radiation ($\lambda = 0.71073\text{ \AA}$). Single crystals of $\text{Cp}^{\text{P}}_3\text{U}$, $\text{Cp}^{\text{P}}\text{UI}_2(\text{THF})_3$, **1-Cp^P**, **2-Cp^P**, **4-Cp***, **5-Cp^P**, and **5-Cp*** suitable for X-ray diffraction were coated with poly(isobutylene) oil in a glovebox and quickly transferred to the goniometer head of a Rigaku Rapid II image plate diffractometer equipped with a MicroMax002+ high intensity copper X-ray source with confocal optics. Preliminary examination and data collection were performed with Cu $K\alpha$ radiation ($\lambda = 1.54184\text{ \AA}$). Cell constants for data collection were obtained from least-squares refinement. The space group was identified using the program XPREP.²⁶ The structures were solved using the structure solution program PATTY in DIRDIF99.²⁷ Refinement was performed on a LINUX PC using SHELX-97.²⁶

Magnetic susceptibility (dc) data were collected on compounds **1-Cp^P** and **5-Cp^P** with a Quantum Design MPMS-XL SQUID magnetometer in the temperature range 5–300 K at an applied field of 1000 Oe. Powdered microcrystalline samples were loaded into gelatin capsules in the glovebox, inserted into a straw, and transported to the SQUID magnetometer under dinitrogen. The absence of significant ferromagnetic impurities was confirmed for each sample by observing a linear relationship between magnetization and applied field (0.1–0.7 T) at 100 K (Figure S1). Susceptibility data reproducibility was probed by analyzing several independently synthesized solid samples: the air-sensitivity of the samples results in slight variation of the room temperature μ_{eff} values, but the qualitative temperature dependences of the data are reproducible (Figure S2). Data for representative samples are presented in Figure 6 and discussed in the

text; the identical data presented as the thermal dependence of $\chi_{\text{M}}T$ (cgs units) can be found in Figure S3. Data were corrected for the magnetization of the sample holder by subtracting the susceptibility of an empty container and for diamagnetic contributions of the sample by using Pascal's constants.²⁸

Synthesis of $\text{Cp}^*\text{UI}_2(\text{MesPDI}^{\text{Me}})$ (1-Cp***).** A 20 mL scintillation vial was charged with 0.788 g (0.934 mmol) of $\text{Cp}^*\text{UI}_2(\text{THF})_3$ and 5 mL of toluene. While stirring, 0.372 g (0.935 mmol) of $\text{MesPDI}^{\text{Me}}$ was added, resulting in a gradual color change from blue to brown. After stirring for 2 h, volatiles were removed *in vacuo*. The resulting solid was washed with cold pentane ($3 \times 10\text{ mL}$) to afford brown solid (0.868 g, 0.847 mmol, 91%) assigned as $\text{Cp}^*\text{UI}_2(\text{MesPDI}^{\text{Me}})$. Elemental analysis of $\text{C}_{37}\text{H}_{46}\text{N}_3\text{I}_2\text{U}$, calculated: C, 43.37; H, 4.53; N, 4.10. Found: C, 43.30; H, 4.52; N, 3.98. ^1H NMR (C_6D_6 , $25\text{ }^{\circ}\text{C}$): δ –68.18 (91, 1H, 4-pyr-ArH), –22.61 (16, 12H, *o*-CH₃), –4.03 (3, 4H, *m*-ArH), –3.98 (3, 6H, CH₃), 12.23 (23, 15H, Cp*), 21.50 (14, 2H, 3,5-pyr-ArH), 31.05 (115, 6H, CH₃).

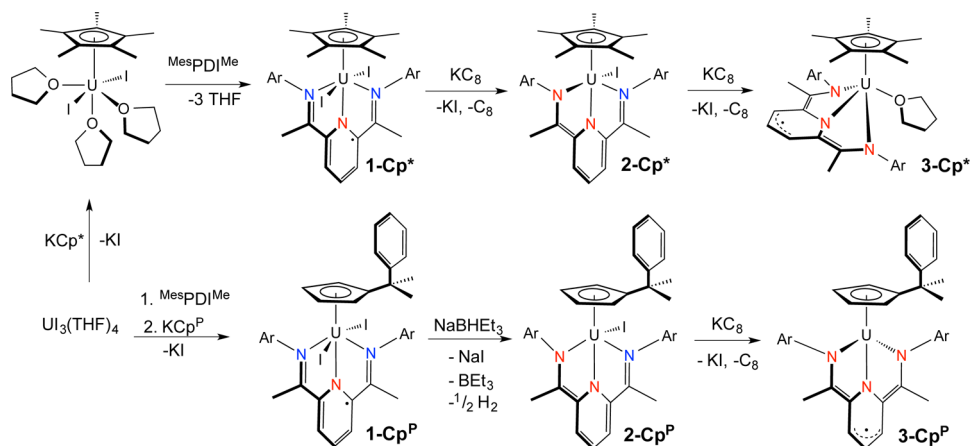
Synthesis of $\text{Cp}^*\text{UI}(\text{MesPDI}^{\text{Me}})$ (2-Cp***).** A 20 mL scintillation vial was charged with 1.000 g (0.976 mmol) of $\text{Cp}^*\text{UI}_2(\text{MesPDI}^{\text{Me}})$ and 10 mL of toluene. While stirring, 0.135 g (0.999 mmol) of KC_8 was added. After 30 min, the dark green solution was filtered over Celite, and volatiles were removed *in vacuo*. The resulting solid was washed with cold pentane ($3 \times 10\text{ mL}$) to afford a dark green solid (0.693 g, 0.772 mmol, 79%) assigned as $\text{Cp}^*\text{UI}(\text{MesPDI}^{\text{Me}})$. Single, X-ray-quality crystals were obtained by slow diffusion of hexane into a saturated toluene solution at $-35\text{ }^{\circ}\text{C}$. Elemental analysis of $\text{C}_{37}\text{H}_{46}\text{N}_3\text{IU}$, calculated: C, 49.50; H, 5.16; N, 4.68. Found: C, 49.46; H, 5.09; N, 4.62. ^1H NMR (C_6D_6 , $25\text{ }^{\circ}\text{C}$): δ –2.21 (5, 6H, CH₃), 0.91 (3, 6H, CH₃), 1.83 (d, $J = 8$, 2H, 3,5-pyr-ArH), 2.00 (3, 6H, CH₃), 2.56 (4, 15H, Cp*), 6.16 (5, 2H, ArH), 7.32 (5, 2H, ArH), 7.43 (5, 6H, CH₃), 7.96 (t, $J = 8$, 1H, 4-pyr-ArH).

Alternate Synthesis of $\text{Cp}^*\text{UI}(\text{MesPDI}^{\text{Me}})(\text{THF})$ (3-Cp***).** A 20 mL scintillation vial was charged with 0.100 g (0.111 mmol) of $\text{Cp}^*\text{UI}(\text{MesPDI}^{\text{Me}})$ and 5 mL of THF. While stirring, 0.016 g (0.118 mmol) of KC_8 was added, and the solution color changed from dark green to brown. After 1 h, the volatiles were removed *in vacuo*. The product was extracted with diethyl ether and filtered over Celite, affording a dark brown solid (0.079 g, 0.094 mmol, 84%) identified as $\text{Cp}^*\text{UI}(\text{MesPDI}^{\text{Me}})(\text{THF})$ by ^1H NMR spectroscopy.

Synthesis of $\text{Cp}_3^{\text{P}}\text{U}$. A 20 mL scintillation vial was charged with 0.340 g (0.375 mmol) of $\text{UI}_3(\text{THF})_4$ and 10 mL of THF. While stirring, 0.249 g (1.124 mmol) of KCp^{P} was added and stirred for 3 h, resulting in a green solution. Volatiles were removed *in vacuo*. The product was extracted with diethyl ether and filtered through Celite. Removal of volatiles afforded a green solid (0.265 g, 0.337 mmol, 90%) assigned as $\text{Cp}_3^{\text{P}}\text{U}$. Single, X-ray quality crystals were grown in a concentrated diethyl ether solution at $-35\text{ }^{\circ}\text{C}$. Elemental analysis of $\text{C}_{42}\text{H}_{45}\text{U}$, calculated: C, 64.03; H, 5.76. Found: C, 63.60; H, 5.82. ^1H NMR (C_6D_6 , $25\text{ }^{\circ}\text{C}$): δ –22.21 (38, 6H, ArH), –13.85 (12, 18H, CH₃), –11.08 (24, 6H, ArH), –2.39 (22, 6H, ArH), 2.70 (21, 3H, *p*-phenyl-ArH), 3.76 (34, 6H, ArH).

Synthesis of $\text{Cp}^{\text{P}}\text{UI}_2(\text{THF})_3$. A 20 mL scintillation vial was charged with 0.335 g (0.369 mmol) of $\text{UI}_3(\text{THF})_4$ and 10 mL of THF and cooled to $-35\text{ }^{\circ}\text{C}$. While stirring, 0.082 g (0.369 mmol) of KCp^{P} was added and stirred for 3 h, resulting in a blue solution. Volatiles were removed *in vacuo*. The product was extracted with diethyl ether and filtered through Celite. Removal of volatiles afforded a blue solid (0.265 g, 0.297 mmol, 81%) assigned as $\text{Cp}^{\text{P}}\text{UI}_2(\text{THF})_3$. Single, X-ray quality crystals were grown in a concentrated diethyl ether solution at $-35\text{ }^{\circ}\text{C}$. Elemental analysis of $\text{C}_{26}\text{H}_{39}\text{I}_2\text{O}_3\text{U}$, calculated: C, 35.03; H, 4.41. Found: C, 34.83; H, 4.31. ^1H NMR (C_6D_6 , $25\text{ }^{\circ}\text{C}$): δ –24.06 (20, 2H, ArH), –8.26 (16, 2H, ArH), –5.53 (36, 1H, Cp^{P} -*p*-phenyl-ArH), –2.36 (548, 6H, Cp^{P} -CH₃), 0.67 (294, 24H, THF-CH₂), 4.79 (45, 2H, ArH), 9.54 (85, 2H, ArH).

Synthesis of $\text{Cp}^{\text{P}}\text{UI}_2(\text{MesPDI}^{\text{Me}})$ (1-Cp^P**).** A 20 mL scintillation vial was charged with 0.469 g (0.517 mmol) of $\text{UI}_3(\text{THF})_4$, 0.205 g (0.516 mmol) of $\text{MesPDI}^{\text{Me}}$, and 15 mL of toluene and stirred for 15 min. Volatiles were removed, affording a brown solid. The solid was redissolved in 15 mL of toluene. While stirring, 0.115 g (0.518 mmol) of KCp^{P} was added and allowed to stir for 30 min. The brown

Scheme 1. Synthesis of $\text{Mes}^*\text{PDI}^{\text{Me}}$ Uranium Derivatives

suspension was filtered over Celite, and volatiles were removed *in vacuo* to yield a brown solid (0.553 g, 0.516 mmol, 95%) assigned as $\text{Cp}^*\text{UI}_2(\text{Mes}^*\text{PDI}^{\text{Me}})$. Single, X-ray quality crystals were obtained from a concentrated toluene/pentane (10:1) solution at -35°C . Elemental analysis of $\text{C}_{41}\text{H}_{46}\text{N}_3\text{I}_2\text{U}$, calculated: C, 45.91; H, 4.32; N, 3.92. Found: C, 45.93; H, 4.42; N, 3.82. $^1\text{H NMR}$ (C_6D_6 , 25°C): δ -47.26 (27, 2H, ArH), -18.20 (12, 12H, *o*- CH_3), -5.55 (10, 6H, CH_3), -3.05 (3, 3H, $\text{Cp}^*\text{-CH}_3$), -2.83 (7, 3H, $\text{Cp}^*\text{-CH}_3$), -0.83 (3, 1H, ArH), 11.18 (t, $J = 8$, 1H, ArH), 12.91 (t, $J = 8$, 2H, $\text{Cp}^*\text{-ArH}$), 13.38 (34, 2H, ArH), 17.40 (74, 6H, CH_3), 17.95 (11, 2H, ArH), 18.73 (42, 4H, $\text{PDI-}m\text{-ArH}$), 21.81 (d, $J = 8$, 2H, ArH).

Synthesis of $\text{Cp}^*\text{UI}(\text{Mes}^*\text{PDI}^{\text{Me}})$ (2- Cp^*). A 20 mL scintillation vial was charged with 1.072 g (1.000 mmol) of $\text{Cp}^*\text{UI}_2(\text{Mes}^*\text{PDI}^{\text{Me}})$ and 15 mL of toluene. While stirring, 1.00 mL (1.000 mmol) of NaHBET_3 solution (1.0 M in toluene) was added, resulting in H_2 evolution as indicated by bubbling. After stirring for 15 min, the dark brown suspension was filtered over Celite. Volatiles were removed *in vacuo* to afford a dark brown solid (0.912 g, 0.964 mmol, 97%) assigned as $\text{Cp}^*\text{UI}(\text{Mes}^*\text{PDI}^{\text{Me}})$. Single, X-ray quality crystals were obtained from a concentrated toluene/pentane (1:3) solution at -35°C . Elemental analysis of $\text{C}_{41}\text{H}_{46}\text{N}_3\text{IU}$, calculated: C, 52.07; H, 4.90; N, 4.44. Found: C, 51.98; H, 5.07; N, 4.39. $^1\text{H NMR}$ (C_6D_6 , 25°C): δ -65.44 (60, 6H, CH_3), -48.48 (59, 6H, CH_3), -16.90 (1, 2H, ArH), -8.73 (12, 2H, ArH), -8.38 (12, 2H, ArH), -3.70 (5, 6H, CH_3), 0.93 (17, 6H, CH_3), 8.37 (606, 4H, $\text{Cp}^*\text{-Ph-}o,p\text{-ArH}$), 18.10 (20, 1H, ArH), 21.90 (24, 2H, ArH), 45.50 (31, 1H, ArH), 47.22 (87, 2H, ArH), 70.01 (54, 3H, CH_3), 73.78 (111, 3H, CH_3).

Synthesis of $\text{Cp}^*\text{U}(\text{Mes}^*\text{PDI}^{\text{Me}})$ (3- Cp^*). A 20 mL scintillation vial was charged with 0.912 g (0.964 mmol) of $\text{Cp}^*\text{UI}(\text{Mes}^*\text{PDI}^{\text{Me}})$ and 15 mL of toluene. While stirring, 0.140 g (1.036 mmol) of KC_8 was added. After stirring for 30 min, the dark brown suspension was filtered over Celite, and volatiles were removed *in vacuo*. The resulting solid was washed with cold pentane (-35°C) to afford a dark brown solid (0.568 g, 0.694 mmol, 72%) assigned as $\text{Cp}^*\text{U}(\text{Mes}^*\text{PDI}^{\text{Me}})$. Elemental analysis of $\text{C}_{41}\text{H}_{46}\text{N}_3\text{U}$, calculated: C, 60.14; H, 5.66; N, 5.13. Found: C, 60.09; H, 5.58; N, 5.08. $^1\text{H NMR}$ (C_6D_6 , 25°C): δ -109.93 (164, 1H, ArH), -65.95 (159, 2H, ArH), -42.93 (321, 6H, CH_3), -27.90 (119, 6H, CH_3), -19.00 (162, 6H, CH_3), -10.20 (22, 2H, ArH), -8.09 (50, 2H, ArH), -1.82 (42, 6H, CH_3), 1.12 (71, 2H, ArH), 17.70 (58, 1H, ArH), 21.53 (94, 2H, ArH), 26.78 (247, 6H, CH_3), 46.73 (189, 2H, ArH), 76.69 (416, 2H, ArH).

Synthesis of $\text{Cp}^*\text{UI}(\text{Furf})$ ($\text{Mes}^*\text{PDI}^{\text{Me}}$) (4- Cp^*). A 20 mL scintillation vial was charged with 0.096 g (0.102 mmol) of $\text{Cp}^*\text{UI}(\text{Mes}^*\text{PDI}^{\text{Me}})$ and 5 mL of toluene and stirred. Furfural (0.0085 mL, 0.101 mmol) was added via microsyringe, resulting in an immediate color change from brown to dark green. Volatiles were then removed, and the resulting solid was washed with pentane (2×10 mL), affording a green solid (0.097 g, 0.093 mmol, 92%) assigned as $\text{Cp}^*\text{UI}(\text{Furf})$ ($\text{Mes}^*\text{PDI}^{\text{Me}}$). Elemental Analysis of $\text{C}_{46}\text{H}_{50}\text{N}_3\text{IOU}$, calculated: C, 53.86; H, 4.91; N, 4.10. Found: C, 53.98; H, 5.09; N, 4.07. ^1H

NMR (C_6D_6 , 25°C): δ -63.30 (127, 1H, ArH), -43.63 (33, 1H, ArH), -23.58 (9, 3H, CH_3), -21.80 (12, 3H, CH_3), -20.57 (17, 3H, CH_3), -12.67 (61, 1H, ArH), -8.01 (21, 1H, ArH), -7.17 (10, 3H, CH_3), -4.99 (8, 1H, ArH), -3.41 (7, 3H, CH_3), -2.66 (7, 3H, CH_3), 3.30 (33, 3H, CH_3), 5.36 (8, 1H, ArH), 5.82 (t, $J = 8$, 1H, $\text{Cp}^*\text{-}p\text{-ArH}$), 5.93 (t, $J = 9$, 1H, ArH), 6.26 (t, $J = 8$, 2H, $\text{Cp}^*\text{-}m\text{-ArH}$), 6.76 (25, 1H, ArH), 6.80 (d, $J = 8$, 2H, $\text{Cp}^*\text{-}o\text{-ArH}$), 6.88 (25, 1H, ArH), 7.42 (d, $J = 8$, 1H, ArH), 10.86 (9, 3H, CH_3), 13.16 (13, 3H, CH_3), 13.51 (8, 1H, ArH), 15.06 (7, 1H, ArH), 17.89 (12, 3H, CH_3), 22.69 (10, 1H, ArH), 42.51 (53, 1H, ArH), 107.80 (40, 1H, ArH).

Synthesis of $\text{Cp}^*\text{UI}(\text{Furf})$ ($\text{Mes}^*\text{PDI}^{\text{Me}}$) (4- Cp^*). A 20 mL scintillation vial was charged with 0.150 g (0.167 mmol) of $\text{Cp}^*\text{UI}(\text{Mes}^*\text{PDI}^{\text{Me}})$ and 5 mL of toluene and stirred. Furfural (0.014 mL, 0.170 mmol) was added via microsyringe, resulting in an immediate color change from green to brown. Volatiles were then removed, and the resulting solid was washed with pentane (2×10 mL), affording a brown solid (0.120 g, 0.093 mmol, 72%) assigned as $\text{Cp}^*\text{UI}(\text{Furf})$ ($\text{Mes}^*\text{PDI}^{\text{Me}}$). Single, X-ray quality crystals were obtained from a concentrated toluene/pentane (2:1) solution at -35°C . Elemental analysis of $\text{C}_{42}\text{H}_{50}\text{N}_3\text{O}_2\text{IU}$, calculated: C, 50.76; H, 5.07; N, 4.23. Found: C, 50.69; H, 5.13; N, 4.09. $^1\text{H NMR}$ (C_6D_6 , 25°C): δ -23.71 (11, 3H, CH_3), -21.13 (8, 3H, CH_3), -16.87 (9, 3H, CH_3), -7.58 (7, 1H, ArH), -7.24 (7, 1H, ArH), -5.81 (9, 3H, CH_3), -4.54 (6, 3H, CH_3), -4.32 (7, 3H, CH_3), -2.81 (d, $J = 8$, 1H, ArH), -0.41 (7, 1H, ArH), 1.45 (9, 15H, Cp^*), 7.37 (t, $J = 8$, 1H, ArH), 8.33 (9, 3H, CH_3), 8.51 (11, 3H, CH_3), 8.78 (t, $J = 6$, 1H, ArH), 10.29 (d, $J = 8$, 1H, ArH), 14.34 (8, 1H, ArH), 15.75 (6, 1H, ArH), 24.38 (10, 1H, ArH), 103.10 (26, 1H, ArH).

Synthesis of $\text{Cp}^*\text{U}(\text{O}_2\text{C}_2\text{Ph}_4)$ ($\text{Mes}^*\text{PDI}^{\text{Me}}$) (5- Cp^*). A 20 mL scintillation vial was charged with 0.095 g (0.116 mmol) of $\text{Cp}^*\text{U}(\text{Mes}^*\text{PDI}^{\text{Me}})$ and 5 mL of toluene. While stirring, 0.043 g (0.236 mmol) of benzophenone was added. After 15 min, volatiles were removed *in vacuo*. The resulting solid was washed with cold pentane (-35°C) to afford a dark brown solid (0.099 g, 0.084 mmol, 72%) assigned as $\text{Cp}^*\text{U}(\text{O}_2\text{C}_2\text{Ph}_4)$ ($\text{Mes}^*\text{PDI}^{\text{Me}}$). Single, X-ray quality crystals were grown by slow diffusion of *n*-hexane into a concentrated THF solution at -35°C . Elemental analysis of $\text{C}_{67}\text{H}_{66}\text{N}_3\text{O}_2\text{U}$, calculated: C, 68.01; H, 5.62; N, 3.55. Found: C, 67.72; H, 5.64; N, 3.43. $^1\text{H NMR}$ (C_6D_6 , 25°C): δ -310.96 (76, 1H, ArH), -25.28 (9, 2H, ArH), -7.14 (24, 6H, CH_3), -1.51 (24, 6H, CH_3), 3.20 (d, $J = 8$, 2H, *o*-ArH), 3.66 (12, 6H, CH_3), 5.76 (t, $J = 8$, 2H, *m*-ArH), 5.91 (t, $J = 6$, 1H, *p*-ArH), 6.68 (646, 8H, $\text{O}_2\text{C}_2\text{Ph}_4\text{-ArH}$), 7.67 (779, 4H, $\text{O}_2\text{C}_2\text{Ph}_4\text{-}p\text{-ArH}$), 8.93 (277, 8H, $\text{O}_2\text{C}_2\text{Ph}_4\text{-ArH}$), 12.04 (7, 2H, ArH), 13.53 (12, 2H, ArH), 15.77 (23, 6H, CH_3), 25.51 (12, 2H, ArH), 38.14 (15, 2H, ArH), 177.43 (72, 6H, CH_3).

Synthesis of $\text{Cp}^*\text{U}(\text{O}_2\text{C}_2\text{Ph}_2\text{H}_2)$ ($\text{Mes}^*\text{PDI}^{\text{Me}}$) (5- Cp^*). A 20 mL scintillation vial was charged with 0.220 g (0.261 mmol) of $\text{Cp}^*\text{U}(\text{Mes}^*\text{PDI}^{\text{Me}})(\text{THF})$ and 5 mL of toluene and frozen. Upon thawing, 0.053 mL (0.522 mmol) of benzaldehyde was added via microsyringe. The reaction was stirred for 2 h, and volatiles were

removed. The crude mixture was recrystallized by slow evaporation of a concentrated diethyl ether solution to afford a green solid (0.123 g, 0.125 mmol, 48%) assigned as $\text{Cp}^*\text{U}(\text{O}_2\text{C}_2\text{Ph}_2\text{H}_2)(^{\text{Mes}}\text{PDI}^{\text{Me}})$. Single, X-ray quality crystals were grown from a concentrated toluene/pentane solution (4:1) at -35°C . Elemental analysis of $\text{C}_{51}\text{H}_{58}\text{N}_3\text{O}_2\text{U}$, calculated: C, 62.31; H, 5.95; N, 4.27. Found: C, 62.23; H, 6.10; N, 4.24. ^1H NMR (C_6D_6 , 25°C): δ -50.93 (15, 2H, ArH), -49.52 (16, 2H, ArH), -23.81 (24, 2H, ArH), -22.17 (22, 2H, ArH), -19.85 (d, $J = 24$, 1H, Pin-CH), -5.91 (10, 1H, ArH), -5.71 (8, 1H, ArH), -5.49 (7, 1H, ArH), -5.26 (d, $J = 11$, 1H, Pin-CH), 1.54 (6, 1H, ArH), 1.95 (5, 6H, CH_3), 2.09 (7, 6H, CH_3), 2.14 , (7, 6H, CH_3), 3.80 (11, 1H, ArH), 9.67 (32, 1H, ArH), 9.85 (36, 1H, ArH), 12.98 (11, 15H, Cp^*), 19.63 (17, 3H, CH_3), 22.40 (17, 3H, CH_3).

Reactivity of 3- Cp^* with Benzaldehyde. A 20 mL scintillation vial was charged with 0.027 g (0.033 mmol) of $\text{Cp}^*\text{U}(\text{MesPDI}^{\text{Me}})$ and 3 mL of toluene. While stirring, benzaldehyde (6.7 μL , 0.066 mmol) was added via microsyringe. After 30 min without a noticeable color change, volatiles were removed *in vacuo*. Inspection by ^1H NMR spectroscopy revealed decomposition of the starting material without significant consumption of benzaldehyde.

Reactivity of 3- Cp^* with Benzophenone. A 20 mL scintillation vial was charged with 0.035 g (0.042 mmol) of $\text{Cp}^*\text{U}(\text{MesPDI}^{\text{Me}})$ (THF) and 3 mL of toluene. While stirring, benzophenone (0.016 g, 0.088 mmol) was added, resulting in an immediate color change from brown to dark red. After 10 min, volatiles were removed. Inspection by ^1H NMR spectroscopy revealed significant decomposition of starting material without consumption of benzophenone.

RESULTS AND DISCUSSION

Synthesis of Reduced Species. Initial studies focused on metalation of $^{\text{Mes}}\text{PDI}^{\text{Me}}$ for the synthesis of a series of reduced Cp^* uranium derivatives. Treating a stirring blue toluene solution of $\text{Cp}^*\text{UI}_2(\text{THF})_3$ with one equivalent of $^{\text{Mes}}\text{PDI}^{\text{Me}}$ resulted in a color change to brown over a 3 h period (Scheme 1, red = anionic bond, blue = dative bond). Following the workup, analysis by ^1H NMR spectroscopy revealed seven paramagnetically shifted resonances, suggesting metalation and formation of C_{2v} symmetric $\text{Cp}^*\text{UI}_2(^{\text{Mes}}\text{PDI}^{\text{Me}})$ (**1- Cp^***), with an intense singlet at 12.23 ppm assigned as the $\eta^5\text{-Cp}^*$ ligand.

Reduction of **1- Cp^*** was achieved by treatment with one equivalent of KC_8 (Scheme 1). Following the workup, analysis of the isolated dark green solid by ^1H NMR spectroscopy revealed nine paramagnetically broadened resonances spanning from -2.21 to 7.96 ppm with the largest at 2.56 ppm assigned as the $\eta^5\text{-Cp}^*$. Four resonances integrating to six protons each corresponding to pairs of methyl groups on the $^{\text{Mes}}\text{PDI}^{\text{Me}}$ ligand signify a C_s symmetric complex in solution, $\text{Cp}^*\text{UI}(\text{MesPDI}^{\text{Me}})$ (**2- Cp^***).

Structural confirmation and features of **2- Cp^*** were elucidated by crystallographic analysis of single, X-ray-quality crystals obtained from the slow diffusion of hexane into a saturated toluene solution at -35°C (Figure 1, Table 1). Refinement of the data revealed the uranium iodide complex with both $\eta^5\text{-Cp}^*$ and $^{\text{Mes}}\text{PDI}^{\text{Me}}$ ligands. The U1–I1 and U–Ct distances (3.1087(8) and 2.386 Å, respectively) are on the order of those for $\text{Cp}^*\text{UI}_2(\text{NCCH}_3)$ (3.07(2) and 2.465 Å).²⁹ The uranium center is situated 1.189 Å above the $^{\text{Mes}}\text{PDI}^{\text{Me}}$ N–N–N plane.

Intraligand distances have been established as an important metric for determining pyridine (diimine) ligand reduction.^{30–32} A comparison of ligand bond distances in **2- Cp^*** as compared to free $^{\text{Mes}}\text{PDI}^{\text{Me}}$ confirms localized ligand reduction. The N1–C2 distance of 1.454(12) Å is severely elongated compared to that in the free ligand of 1.277(3) Å (Figure S5), whereas the C2–C3 bond of 1.386(13) Å is contracted versus $^{\text{Mes}}\text{PDI}^{\text{Me}}$

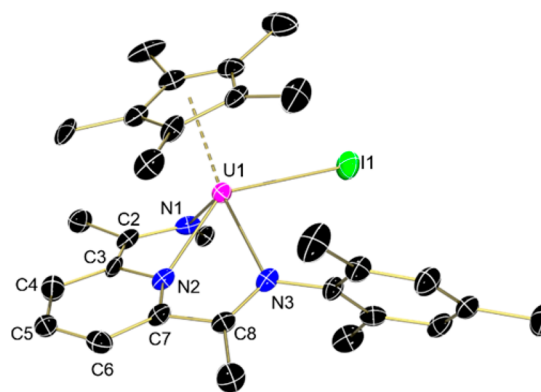


Figure 1. Molecular structure of $\text{Cp}^*\text{UI}(\text{MesPDI}^{\text{Me}})$ (**2- Cp^***) shown with 30% probability ellipsoids. Hydrogen atoms as well as one 2,4,6-trimethylphenyl substituent have been omitted for clarity.

(1.495(3) Å). On the other hand, the C7–C8 distance of 1.499(12) Å is very close to the free ligand value, indicating no reduction for this bond, and very little for N3–C8 (1.349(11) Å) as well (1.349(11) Å). Thus, reduction appears to be relegated to one part of the ligand in the molecular structure.

This is further evident from inspection of the uranium–nitrogen bond distances for $^{\text{Mes}}\text{PDI}^{\text{Me}}$. Although not as thoroughly studied, these U–N distances are a more reliable parameter for establishing ligand reduction due to the higher accuracy in these measurements. In **2- Cp^*** , the long U1–N3 distance of 2.781(8) Å is consistent with a dative interaction, as would be expected for a neutral $[\text{MesPDI}^{\text{Me}}]^0$. Upon ligand reduction, however, the U–N bonds change in character from dative to monoanionic, which is highlighted by bond shortening. Thus, the U1–N2 and U1–N1 bond distances of 2.337(8) and 2.156(8) Å, respectively, are on the order of uranium amides^{33–35} and support reduction on this side of the ligand in the solid state. Taken with the intraligand distances, the metric parameter for **2- Cp^*** supports a dianionic, $[\text{MesPDI}^{\text{Me}}]^{2-}$. The distances in **2- Cp^*** are also reminiscent of those in $(^{\text{Mes}}\text{DAB}^{\text{Me}})_2\text{U}(\text{THF})$ ($^{\text{Mes}}\text{DAB}^{\text{Me}} = [\text{ArN}=\text{C}(\text{Me})-\text{C}(\text{Me})=\text{NAr}]$, Ar = 2,4,6-trimethylphenyl (Mes)), which has been characterized to have dianionic $[\text{MesDAB}^{\text{Me}}]^{2-}$ ligands.³⁶

By analogy to the reduction of **1- Cp^*** , treating **2- Cp^*** with one equivalent of KC_8 resulted in ligand reduction to generate $\text{Cp}^*\text{U}(\text{MesPDI}^{\text{Me}})(\text{THF})$ (**3- Cp^***). Compound **3- Cp^*** was previously synthesized by the addition of 2 equiv of KC_8 to a solution of $\text{Cp}^*\text{UI}_2(\text{THF})$ and $^{\text{Mes}}\text{PDI}^{\text{Me}}$ (1:1). The former synthetic route to **3- Cp^*** from **2- Cp^*** resulted in similar purity and yields (84%) to the latter but circumvents the loss of a Cp^* ligand. Compound **3- Cp^*** is established to have a triply reduced $[\text{MesPDI}^{\text{Me}}]^{3-}$ ligand,¹⁹ demonstrating that reduction occurs at $^{\text{Mes}}\text{PDI}^{\text{Me}}$ and not the uranium center.

With the Cp^* reduction series in hand, synthesis of the same series using the less sterically demanding 1-(7,7-dimethylbenzyl)cyclopentadienyl (Cp^{P}) ligand was attempted. Synthesis of $\text{Cp}^{\text{P}}\text{UI}_2(\text{THF})_x$ was targeted first as an entry into the reduction series by analogy to $\text{Cp}^*\text{UI}_2(\text{THF})_3$ ²² and was possible by the addition of a single equivalent of KCp^{P} to a THF solution of $\text{UI}_3(\text{THF})_4$. Following the workup, the blue solid showed a paramagnetically shifted ^1H NMR spectrum with broad resonances, most likely due to the dynamic nature of the Cp^{P} ring in solution. Seven signals spanning from -24.06 to 9.54 ppm were observed, including a resonance at -2.36 ppm for the equivalent methyl protons (6H) and a broad

Table 1. Bond Distances (Å) for $^{\text{Mes}}\text{PDI}^{\text{Me}}$, 2-Cp^{P} , 1-Cp^{P} , 2-Cp^{P} , and $\text{Cp}^{\text{P}}\text{UI}_2(\text{THF})_3$

	$^{\text{Mes}}\text{PDI}^{\text{Me}}$	X=N			X=O
		2-Cp^{P}	1-Cp^{P}	2-Cp^{P}	$\text{Cp}^{\text{P}}\text{UI}_2(\text{THF})_3$
U–X1		2.156(8)	2.522(10)	2.500(2)	2.500(12)
U–X2		2.337(8)	2.368(10)	2.234(3)	2.569(14)
U–X3		2.781(8)	2.484(9)	2.327(3)	2.490(11)
N1–C2	1.277(3)	1.454(12)	1.331(16)	1.317(4)	
C2–C3	1.495(3)	1.386(13)	1.480(18)	1.441(4)	
C3–C4	1.386(3)	1.509(13)	1.334(16)	1.357(5)	
C4–C5	1.378(3)	1.353(13)	1.384(17)	1.404(5)	
C5–C6	1.383(3)	1.375(13)	1.387(18)	1.354(5)	
C6–C7	1.388(3)	1.426(11)	1.393(16)	1.416(5)	
N2–C3	1.346(2)	1.379(11)	1.407(15)	1.409(4)	
N2–C7	1.343(3)	1.362(11)	1.385(14)	1.427(4)	
C7–C8	1.494(3)	1.499(12)	1.434(16)	1.378(5)	
N3–C8	1.276(3)	1.349(11)	1.325(14)	1.375(4)	
U–Ct		2.386	2.500	2.492	2.505
U–I1		3.1087(8)	3.1257(9)	3.0326(3)	3.1667(16)
U–I2			3.0318(10)		3.1562(19)

^aThe free ligand, $^{\text{Mes}}\text{PDI}^{\text{Me}}$, is shown for comparison.

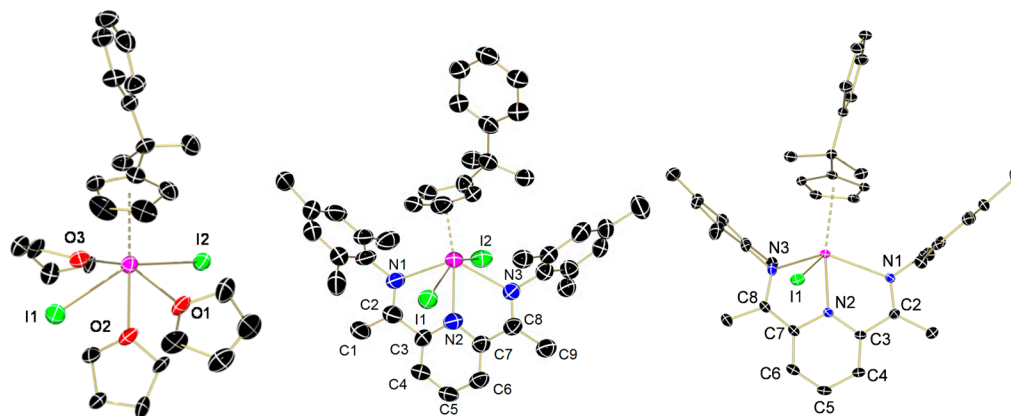


Figure 2. Molecular structures of $\text{Cp}^{\text{P}}\text{UI}_2(\text{THF})_3$ (left), 1-Cp^{P} (middle), and 2-Cp^{P} (right) shown with 30% probability ellipsoids. Hydrogen atoms and cocrystallized solvent molecules are omitted for clarity.

singlet ($\Delta_{1/2} = 294$) at 0.67 ppm assigned as coordinated THF molecules.

X-ray crystallography was employed to elucidate the structure and determine the number of coordinated solvent molecules in $\text{Cp}^{\text{P}}\text{UI}_2(\text{THF})_x$. Refinement of the data from single crystals grown from diethyl ether at $-35\text{ }^\circ\text{C}$ confirmed the product as $\text{Cp}^{\text{P}}\text{UI}_2(\text{THF})_3$ (Figure 2, left; Table 1). The molecular structure shows $\text{Cp}^{\text{P}}\text{UI}_2(\text{THF})_3$ has a U–C_{centroid} distance of 2.505 Å and U–I distances of 3.1667(16) and 3.1562(19) Å, which are all within range for other uranium(III) cyclopentadienyl complexes.^{22,37,38} The phenyl group of the Cp^{P} ring points away from the uranium center, while the two adjacent methyl groups are angled toward it.

Using similar conditions to those established for the synthesis of 1-Cp^{P} , $\text{Cp}^{\text{P}}\text{UI}_2(\text{THF})_3$ was treated with one equivalent of $^{\text{Mes}}\text{PDI}^{\text{Me}}$ to generate $\text{Cp}^{\text{P}}\text{UI}_2(^{\text{Mes}}\text{PDI}^{\text{Me}})$ (1-Cp^{P}). While analysis by ^1H NMR spectroscopy did show a product with the expected number of resonances and symmetry for 1-Cp^{P} , inseparable side products were also formed. Attempts to isolate pure 1-Cp^{P} by varying solvents and reaction times were unsuccessful.

With the inability to generate 1-Cp^{P} cleanly, direct synthesis of 3-Cp^{P} was attempted in an analogous manner to 3-Cp^{P} ,¹⁹

requiring formation of $\text{Cp}^{\text{P}}_2\text{UI}(\text{THF})_x$. Attempts to generate this by adding two equivalents of KCp^{P} to a THF solution of $\text{UI}_3(\text{THF})_4$ resulted in an immediate color change from purple to green. While analysis of the isolated product by ^1H NMR spectroscopy revealed a paramagnetically shifted spectrum with the six resonances expected for the desired product, X-ray crystallographic analysis of suitable green crystals grown from diethyl ether at $-35\text{ }^\circ\text{C}$ showed the molecular structure to be $\text{Cp}^{\text{P}}_3\text{U}$, rather than $\text{Cp}^{\text{P}}_2\text{UI}(\text{THF})_x$ (Figure S4). The U–C_{centroid} distances range from 2.527 to 2.568 Å and are on the order of those in $[\{1,3\text{-}(\text{Me}_3\text{Si})\text{C}_5\text{H}_3\}_3\text{U}]$ (U–C_{centroid avg} = 2.54 Å).³⁹ Interestingly, the same ^1H NMR spectrum was obtained regardless of whether two or three equivalents of KCp^{P} were used, but $\text{Cp}^{\text{P}}_3\text{U}$ is most efficiently synthesized (90% yield) by the addition of three equivalents of KCp^{P} to $\text{UI}_3(\text{THF})_4$. Attempts to use $\text{Cp}^{\text{P}}_3\text{U}$ for the synthesis of 3-Cp^{P} were unsuccessful.

Synthesis of 1-Cp^{P} was finally possible by the addition of one equivalent of $^{\text{Mes}}\text{PDI}^{\text{Me}}$ to a stirring toluene solution of $\text{UI}_3(\text{THF})_4$, which resulted in an immediate color change from purple to brown (Scheme 1). Following removal of the volatiles, the resulting brown solid was redissolved in toluene and treated with an equivalent of KCp^{P} , causing a color change

from dark brown to orange-brown. The desired product, **1-Cp^P**, was isolated in 95% yield; however, failure to remove volatiles following the addition of ^{Mes}PDI^{Me} led to a lower yield and mixture of products. Analysis of **1-Cp^P** by ¹H NMR spectroscopy showed 13 paramagnetically shifted peaks ranging from -47.26 to 21.81 ppm. A large resonance at -18.20 ppm integrating to 12 protons was assigned as *o*-CH₃ mesityl protons of ^{Mes}PDI^{Me}, and the presence of five more resonances for this ligand indicated a symmetric ^{Mes}PDI^{Me} ligand for **1-Cp^P**.

To confirm the assignment as Cp^PUI₂(^{Mes}PDI^{Me}) (**1-Cp^P**), analysis of a single crystal grown from toluene/pentane (10:1) at -35 °C by X-ray crystallography was performed. Refinement of the data revealed the structure to be the pyridine(diimine) uranium bis(iodide) species with the expected η⁵-Cp^P ligand (Figure 2, middle; Table 1). The iodides are oriented *trans* with respect to each other, with an angle of 153.9(4)°, and have U–I distances of 3.1257(9) and 3.0318(10) Å, similar to those reported for UI₃(THF)₄ (3.103(2)–3.167(2) Å).⁴⁰ The uranium center in **1-Cp^P** sits 0.023 Å above the N–N–N plane of ^{Mes}PDI^{Me}.

Although the intraligand distances are not reliable for ligand oxidation state assignment, as in the case of **2-Cp^{*}**, the U–N distances provide a reliable metric for gauging ligand reduction. For ^{Mes}PDI^{Me} in **1-Cp^P**, there are two long U–N_{imine} distances of 2.522(10) (U1–N1) and 2.484(9) Å (U1–N3), which are assigned as dative bonds and are similar to those reported for the neutral ligand in Cp^{*}U(^{Mes}PDI^{Me})(NPh)₂ of 2.578(5), 2.537(5), and 2.606(5) Å.¹⁹ However, a shorter U1–N2 distance of 2.368(10) Å, similar to those of 2.201(3) for the trianionic chelate in **3-Cp^{*}**,¹⁹ signifies the ligand has been reduced by the uranium(III) center upon coordination, generating [^{Mes}PDI^{Me}]¹⁻ supported by a uranium(IV) center.

Variable temperature magnetic susceptibility studies were performed on **1-Cp^P** to further confirm the ligand oxidation state. The ambient temperature magnetic susceptibility for **1-Cp^P** (μ_{eff} : 3.12 μ_{B}) is significantly lower than that calculated with the Landé formula for either *bona fide* U(III) (⁴I_{9/2}, 3.62 μ_{B}) or U(IV) ions (³H₄, 3.58 μ_{B}), respectively; however, it is in the range observed for complexes in either formal oxidation state. Compound **1-Cp^P** shows qualitatively similar magnetic behavior (Figure 3), with gradual and monotonic decreases in μ_{eff} as the temperature decreases, with a slightly steeper downturn below 20 K. At 5 K, the effective magnetic moment for **1-Cp^P** is 1.25 μ_{B} . The low temperature moment is significantly smaller than that observed in true U(III) complexes (2.5–3 μ_{B} at 2 K)^{41–44} and larger than found in unambiguously U(IV) complexes (0.4–0.8 μ_{B} at 2 K) with orbital singlet ground states.^{45,46} In the scenario where the excited spins of a U(IV) ion couple antiferromagnetically with a ligand-centered radical anion, we might expect the low-temperature effective moment to be somewhat smaller than the 1.73 μ_{B} value calculated for an *S* = 1/2, *g* = 2 spin center. Thus, the data are consistent with a formal U(IV), 5f² site weakly interacting with a ligand radical.

Following successful metalation of ^{Mes}PDI^{Me}, the reduction chemistry of **1-Cp^P** was probed. While multiple reagents were effective for reduction, the addition of a single equivalent of sodium triethylborohydride to a stirring toluene solution of **1-Cp^P** gave the cleanest product in highest yields.⁴⁷ Evolution of H₂ as indicated by effervescence and a darkening of the solution was noted over the course of the reaction. Following the work up, analysis by ¹H NMR spectroscopy showed a new product with 14 paramagnetically shifted resonances ranging from

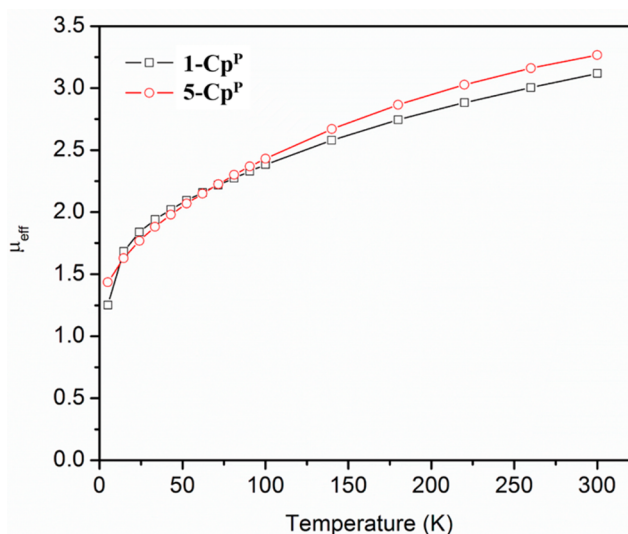


Figure 3. Effective magnetic moment (versus temperature) for **1-Cp^P** and **5-Cp^P**. Susceptibility data were collected at a 1000 Oe measuring field.

–65.44 to 73.78 ppm. Similar to **2-Cp^{*}**, four resonances integrating to six protons each were observed, indicating a C_s symmetric molecule in solution and leading to the preliminary assignment as Cp^PUI(^{Mes}PDI^{Me}) (**2-Cp^P**).

X-ray quality crystals of **2-Cp^P** obtained from a concentrated toluene/pentane (1:3) solution at -35 °C were analyzed. Refinement of the data confirmed the pyridine(diimine) uranium iodide complex with an η⁵-Cp^P ligand (U1–Ct = 2.492 Å; Figure 2, right; Table 1). The U1–I1 bond distance of 3.032(3) Å is within error of other U(IV) complexes with iodide ligands.^{24,29} The uranium center sits 0.815 Å above the plane of ^{Mes}PDI^{Me}. For the pyridine(diimine) chelate, ligand reduction is evident from examination of the intraligand bond distances in **2-Cp^P**. These data highlight a notable difference between the two C–N_{imine} distances, where the N1–C2 distance of 1.317(4) Å is significantly shorter than for N3–C8 of 1.375(4) Å. Thus, while the former maintains double bond character, the latter has undergone reduction. This is confirmed by the adjacent carbon–carbon bond distances, where C2–C3 (1.441(4) Å) is similar to free ^{Mes}PDI^{Me}, and C7–C8 (1.378(5) Å) is contracted due to reduction. Alternating short (C3–C4 and C5–C6) and long (C4–C5 and C6–C7) distances in the pyridine ring signify a loss of aromaticity which can accompany a doubly reduced closed shell ligand.⁴⁸ Therefore, **2-Cp^P** displays a greater extent of ligand reduction as compared to **1-Cp^P**, supporting a ligand based reduction event and formation of dianionic [^{Mes}PDI^{Me}]²⁻ upon exposure to NaHBET₃. Lending further support to this formulation are the U–N bond distances in **2-Cp^P**, where there are two short U–N bonds (U1–N2 = 2.234(3); U1–N3 = 2.327(3) Å) consistent with uranium–amide linkages formed from ligand reduction and one longer U1–N1 bond (2.500(2) Å) for a dative interaction similar to **2-Cp^{*}**.

Further reduction of **2-Cp^P** was attempted to investigate the generation of an analogous compound to **3-Cp^{*}**. The addition of an equivalent of KC₈ to a solution of **2-Cp^P** resulted in the isolation of a dark brown powder. Analysis by ¹H NMR spectroscopy again showed 14 broad, paramagnetically shifted peaks ranging from -109.93 to 76.69 ppm for the C_s symmetric compound. The ¹H NMR data unambiguously establishes the

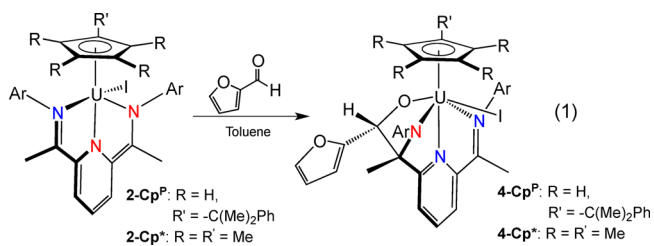
presence of both the Cp^{P} and $^{\text{Mes}}\text{PDI}^{\text{Me}}$ ligands, leading to the assignment as $\text{Cp}^{\text{P}}\text{U}(^{\text{Mes}}\text{PDI}^{\text{Me}})$ (**3-Cp^P**). The absence of additional resonances indicates that no THF is coordinated to the uranium center. While repeated attempts at X-ray crystallographic characterization were unsuccessful, similar spectroscopic features to **3-Cp^{*}** support formulation of this species as containing a $[\text{MesPDI}^{\text{Me}}]^{3-}$ as well.

The uranium derivatives of the Cp^{P} ligand reported here are the first actinide complexes to utilize this framework, as this ligand has previously been used for transition metals^{49–52} and lanthanides.⁵³ For all of the $\text{Cp}^{\text{P}}\text{U}$ complexes, the standard η^5 -coordination mode is the only one observed, in contrast to the titanium(IV) compound, $[\text{Cp}^{\text{P}}\text{Ti}(\text{CH}_3)_2][\text{B}(\text{C}_6\text{F}_5)_4]$, which shows η^6 -coordination of the phenyl ring to the titanium center as well.⁵⁴ The family of reduced uranium complexes of both Cp^{P} and Cp^{P} reported here also highlights the ability of $^{\text{Mes}}\text{PDI}^{\text{Me}}$ to exist in multiple oxidation states, serving to maintain the valency at the uranium center. Additionally, although there are clearly steric and electronic differences of the two cyclopentadienyl ligands, it appears as though there is little influence of the cyclopentadienyl ligand on the ability to isolate analogous species in both series.

Reactivity with Carbonylated Substrates. The isolation of the family of reduced uranium complexes provides an opportunity to determine if the electrons stored in the ligand can be used to promote bond formation or activation reactions. Additionally, the influence of the steric and electronic variability of the cyclopentadienyl ligand on further reactivity can be evaluated. For these studies, C–O bond activation of ketones and aldehydes was explored.

Exposure of **2-Cp^P** to an equivalent of furfural resulted in an immediate color change from brown to green. Infrared spectroscopy showed no absorption assignable to a carbonyl, and analysis by ^1H NMR spectroscopy revealed a complicated (28 resonances) paramagnetically shifted spectrum with peaks ranging from -63 to 107 ppm. Resonances integrating to three ($\times 10$), two ($\times 2$), and single ($\times 16$) protons were identified, indicating an asymmetric molecule in solution, save the Cp^{P} -phenyl protons. These data are consistent with reduction of the carbon–oxygen double bond; however, formation of a stable charge separated ketyl radical product was ruled out as C_s symmetry in solution would be expected for such a species.

The more likely scenario is carbonyl reduction, where the reducing equivalent is derived from $[\text{MesPDI}^{\text{Me}}]^{2-}$, followed by radical coupling of the newly formed ketyl with the remaining $[\text{MesPDI}^{\text{Me}}]^{1-}$, to form $\text{Cp}^{\text{P}}\text{UI}(\text{Furf})(^{\text{Mes}}\text{PDI}^{\text{Me}})$ (**4-Cp^P**) (eq 1).



Radical coupling with reduced carbonyl moieties has been observed for trivalent $\text{Cp}_2^*\text{U}(2,2'\text{-bpy})$ ($2,2'\text{-bpy} = 2,2'$ -bipyridine), which contains a monoanionic bipyridine ligand.⁵⁵ Upon the addition of carbonylated substrates, the carbonyls are reduced by one electron and couple with the bipyridine ligand to generate a family of compounds, $\text{Cp}_2^*\text{U}[(\text{NC}_5\text{H}_4)\text{-NC}_4\text{H}_3\text{CH-CRR}'\text{O}]$ ($\text{R} = \text{R}' = \text{Ph}$; $\text{R} = \text{R}' = \text{Me}$; $\text{R} = \text{H}, \text{R}'$

$= \text{tolyl}$; $\text{R} = \text{H}, \text{R}' = \text{furanyl}$). Unfortunately, single, X-ray-quality crystals of **4-Cp^P** have remained elusive.

Analogous reactivity occurred with the pentamethylcyclopentadienyl complex, **2-Cp^{*}**. Treating a green solution of **2-Cp^{*}** with one equivalent of furfural resulted in an immediate color change to brown (eq 1). Inspection with infrared spectroscopy revealed the disappearance of the carbonyl stretch, and ^1H NMR spectroscopy again revealed a completely asymmetric paramagnetic spectrum ranging from -23 to 103 ppm with a large resonance at 1.45 ppm assigned as the Cp^{P} protons. Eight inequivalent methyl protons from the $^{\text{Mes}}\text{PDI}^{\text{Me}}$ and remaining 11 single-proton resonances led to the product assignment as $\text{Cp}^*\text{UI}(\text{Furf})(^{\text{Mes}}\text{PDI}^{\text{Me}})$ (**4-Cp^{*}**).

Single, X-ray quality crystals of **4-Cp^{*}** obtained from a toluene/pentane solution (2:1, -35 °C) were analyzed to determine the nature of the reductive coupling (Figure 4).

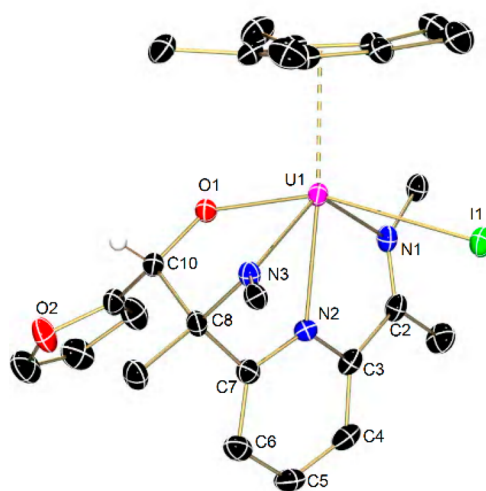
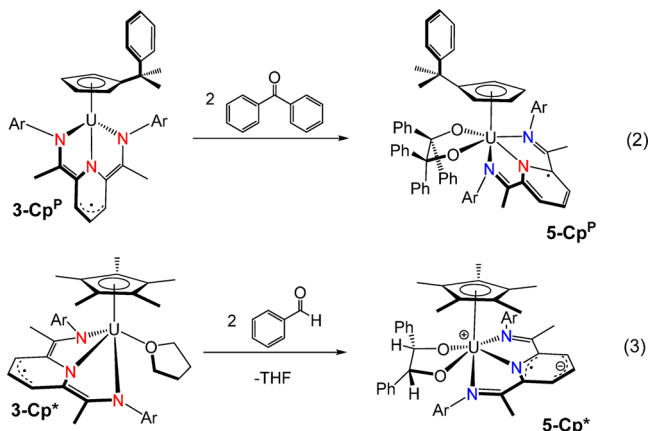


Figure 4. Molecular structure of **4-Cp^{*}** shown with 30% probability ellipsoids. Selected hydrogen atoms, aryl groups, and solvent molecules have been omitted for clarity.

Refinement of the data revealed a uranium iodide supported by an alkoxy-amide $^{\text{Mes}}\text{PDI}^{\text{Me}}$ ligand and capped with an $\eta^5\text{-Cp}^*$ ($\text{U1-Ct} = 2.510$ Å) in a pseudo-octahedral geometry. The molecular structure confirms the carbon–carbon coupling between the furfural ketyl-carbon and the $^{\text{Mes}}\text{PDI}^{\text{Me}}$ imine-carbon ($\text{C8-C10} = 1.575(7)$ Å) and shows the resultant alkoxide ligand is *trans* to the iodide. For the $^{\text{Mes}}\text{PDI}^{\text{Me}}$ ligand, two nitrogens are coordinated to uranium in a dative fashion ($\text{U1-N1} = 2.769(4)$; $\text{U1-N2} = 2.534(2)$ Å), and the other nitrogen has a short U–N bond ($\text{U1-N3} = 2.293(4)$ Å) consistent with an amide linkage. The imine opposite of the coupling shows no reduction ($\text{N1-C2} = 1.283(8)$ Å), and the pyridine ring has rearomatized. The uranium–oxygen distance of $2.137(4)$ Å is as expected for a uranium(IV) alkoxide interaction, while the carbon–oxygen distance of the substrate shows the expected elongation ($\text{O1-C10} = 1.403(6)$ Å) for the reduction to a single bond. The furan ring does not interact with the uranium center. The bond distances account for **4-Cp^{*}** to be in the uranium(IV) oxidation state (as in the starting material, **2-Cp^{*}**), indicating all the redox chemistry has been achieved by use of ligand electrons. Further, weakly intense, sharp transitions ($\epsilon \sim 100 \text{ M}^{-1} \text{ cm}^{-1}$) detected in the near-infrared region for both **4-Cp^P** and **4-Cp^{*}** suggest both metal centers reside in the tetravalent oxidation state (Figure S21).

Complex 4-Cp^{P} displays an intense transition ($\epsilon = 1011 \text{ M}^{-1} \text{ cm}^{-1}$, $\lambda_{\text{max}} = 600 \text{ nm}$) assigned as the color producing band.

Isolation of the analogous $4\text{-Cp}^{\text{P*}}$ and 4-Cp^{P} complexes supports that there is little variation in reactivity between the $\text{Cp}^{\text{P*}}$ and Cp^{P} systems in this case, despite the differences in sterics and electronics. To further probe the role of Cp substituent, the reactivity of the compounds with the triply reduced $^{\text{Mes}}\text{PDI}^{\text{Me}}$ ligands was explored with similar substrates. Treating 3-Cp^{P} with one equivalent of benzophenone



maintained the dark brown solution color (eq 2). Analysis by ^1H NMR spectroscopy showed unreacted starting material as well as the formation of a new product, 5-Cp^{P} , in a 1:1 ratio. To reach full conversion, two equivalents of benzophenone were added to a stirring solution of 3-Cp^{P} , which successfully generated 5-Cp^{P} as the exclusive product. The ^1H NMR spectrum revealed 17 paramagnetically shifted resonances ranging from -310.96 to 177.43 ppm. Deuterium labeling experiments using benzophenone- d_{10} facilitated the assignment of three broad resonances (6.68, 7.67, and 8.93 ppm) corresponding to the protons derived from benzophenone. Analysis of a KBr pellet of 5-Cp^{P} by infrared spectroscopy did not show a carbonyl stretch, supporting reduction of the $\text{C}=\text{O}$

bond. On the basis of the reaction stoichiometry and spectroscopic data, 5-Cp^{P} is assigned as the uranium(IV) pinacolate complex, $\text{Cp}^{\text{P}}\text{U}(\text{O}_2\text{C}_2\text{Ph}_4)(^{\text{Mes}}\text{PDI}^{\text{Me}})$.

To elucidate structural parameters of 5-Cp^{P} , single, X-ray-quality crystals obtained by slow diffusion of *n*-hexane into a concentrated THF solution at -35 °C were analyzed. Refinement of the data confirmed the assignment of 5-Cp^{P} , which is coordinated by pyridine(diimine) and an $\eta^5\text{-Cp}^{\text{P}}$ ligand ($\text{U}1\text{-Ct} = 2.575$ Å; Figure 5, left; Table 2). The U–O

Table 2. Structural Parameters for $4\text{-Cp}^{\text{P*}}$, 5-Cp^{P} , and $5\text{-Cp}^{\text{P*}}$

	$4\text{-Cp}^{\text{P*}}$	5-Cp^{P}	$5\text{-Cp}^{\text{P*}}$
U–N1	2.769(4)	2.679(4)	2.527(3)
U–N2	2.532(4)	2.434(4)	2.523(4)
U–N3	2.293(4)	2.607(4)	2.568(4)
N1–C2	1.283(8)	1.305(6)	1.315(6)
C2–C3	1.493(8)	1.440(7)	1.441(6)
C3–C4	1.389(9)	1.384(7)	1.473(6)
C4–C5	1.372(10)	1.385(8)	1.397(7)
C5–C6	1.377(9)	1.370(8)	1.419(7)
C6–C7	1.400(8)	1.388(7)	1.479(7)
N2–C3	1.345(7)	1.383(7)	1.343(6)
N2–C7	1.340(7)	1.386(7)	1.344(6)
C7–C8	1.509(8)	1.435(7)	1.437(6)
N3–C8	1.492(7)	1.321(6)	1.311(6)
U–Ct	2.510	2.575	2.592
U–O1	2.137(4)	2.118(3)	2.151(3)
U–O2		2.155(3)	2.133(3)
U–H1	3.0860(4)		
C27–C34		1.647(6)	1.554(6)

distances of 2.118(3) and 2.155(3) Å are similar to those found in the uranium(IV) bis(pinacolate), $\text{U}(\text{O}_2\text{C}_2\text{Ph}_4)_2(\text{THF})_2$, reported by Ephritikhine and co-workers.⁵⁶ Due to the extreme steric hindrance in the molecule, the uranium center is pulled out of the plane of the pyridine(diimine) ligand by 1.099 Å.

Examination of the intraligand bond distances indicates that $^{\text{Mes}}\text{PDI}^{\text{Me}}$ is reduced by a single electron in 5-Cp^{P} . In

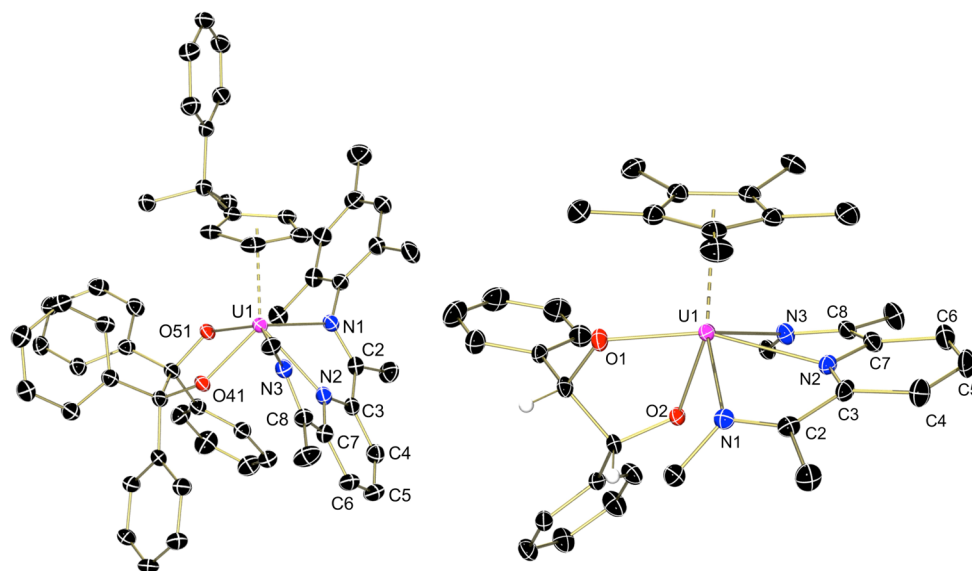


Figure 5. Molecular structure of 5-Cp^{P} (left) and $5\text{-Cp}^{\text{P*}}$ (right) shown with 30% probability ellipsoids. Hydrogen atoms, selected 2,4,6-trimethylphenyl groups, and cocrystallized solvent molecules have been omitted for clarity.

comparison to the free ligand, both C–N_{imine} distances are elongated, while the adjacent C–C distances are contracted, supporting ligand reduction. Furthermore, the N_{pyr}–C distances of 1.383(7) and 1.386(7) Å are elongated as compared to the free ligand but are on the order of those in **1-Cp^P**. This reduction pattern is further evident in the respective U1–N1 and U1–N3 distances of 2.607(4) and 2.679(4) Å for ^{Mes}PDI^{Me} in **5-Cp^P**, which are on the order of dative uranium–nitrogen bonds, while the U1–N2 distance (2.434(4) Å) is shorter, supporting electron occupation of the ligand similar to that in **1-Cp^P** for the assignment as monoanionic [^{Mes}PDI^{Me}]^{1–}.

Formulation of [^{Mes}PDI^{Me}]^{1–} in **5-Cp^P** is further confirmed by variable temperature magnetic susceptibility studies (Figure 3). The ambient temperature magnetic susceptibility of **5-Cp^P** is 3.27 μ_B, which is slightly larger than for **1-Cp^P** (μ_{eff}: 3.12 μ_B) but in the range expected for uranium(III) or (IV) compounds. As in the case of **1-Cp^P**, there is a gradual and monotonic decrease in μ_{eff} for **5-Cp^P** as the temperature decreases, with a final effective magnetic moment of 1.44 μ_B at 5 K. While the low temperature moment is intermediate of U(III) and U(IV) complexes with orbital singlet ground states,^{45,46} based on the similarity to **1-Cp^P**, the low temperature magnetic data are consistent with a formal U(IV), 5f² site weakly interacting with a ligand radical.

The presence of this ligand radical in **5-Cp^P** supports that the two electrons to reduce both equivalents of OCP₂ to [OCP₂][•] were derived from trianionic [^{Mes}PDI^{Me}]^{3–} in **3-Cp^P**. Thus, one reducing equivalent remains and is localized in ^{Mes}PDI^{Me}. Generating radical character in both benzophenone ligands results in radical coupling to form the pinacolate product, **5-Cp^P**, which has been oxidized to a radical [^{Mes}PDI^{Me}]^{1–} ligand and uranium(IV) center. Thus, the tetravalent uranium center is maintained throughout the reaction, with redox events promoted by the ligand.

Radical coupling mediated by electron-rich uranium species is well established, especially for substrates such as CO,⁵⁷ NO,⁵⁸ and diphenylacetylene.¹³ For carbonyl substrates, Ephritikhine reports early examples with the formation of UCl₂(O₂C₂Ph₄) and U(O₂C₂Ph₄)₂(THF)₂ by treating UCl₄ with varying amounts of Na/Hg in the presence of benzophenone.⁵⁶ Meyer demonstrates that trivalent [(^{Ad}ArO)₃tacn]U can reduce benzophenone to form the *transient* uranium(IV) charge separated benzophenone radical species, [(^{Ad}ArO)₃tacn-U^{IV}(OC-Ph₂)].⁵⁹ This species is unstable and can undergo radical coupling either with a second equivalent through the *para*-phenyl carbon of activated benzophenone to form dimeric [(^{Ad}ArO)₃tacn]U^{IV}(OCPhPh–CPh₂O)U^{IV}(^{Ad}ArO)₃tacn] or with an H[•] source to form [(^{Ad}ArO)₃tacn]U^{IV}(OC-Ph₂). Benzaldehyde coupling by Cp₃U(THF) has also been reported, which produced tetravalent Cp₃UOC(Ph)H-PhCHOCp₃U.⁶⁰ Interestingly, **3-Cp^P** was found to decompose when exposed to benzaldehyde, indicating that clean C–O bond activation by **3-Cp^P** cannot be extended to aldehydes.

Reactivity of **3-Cp^{*}** with benzophenone was tested under the same conditions as for **3-Cp^P**. The addition of two equivalents of benzophenone resulted in immediate decomposition of **3-Cp^{*}** without the formation of tractable uranium products. This decomposition is most likely due to the increased steric bulk of the Cp^{*} ligand as compared to Cp^P, which prevents substrate access and formation of the pinacolate derivative. Thus, compound **3-Cp^{*}** was treated with two equivalents of benzaldehyde, which caused an immediate color change from

brown to green (eq 3). ¹H NMR spectroscopy gave a spectrum of a single, paramagnetically shifted product, **5-Cp^{*}**, with a singlet at 12.98 ppm assigned as the equivalent Cp^{*} protons. Analysis of the crude material by IR spectroscopy confirmed the absence of an absorption for a C=O double bond (Figure S20).

To confirm the identity of **5-Cp^{*}**, single, X-ray-quality crystals obtained from a concentrated toluene/pentane (4:1) solution cooled to –35 °C were analyzed. Refinement of the data revealed an η⁵-Cp^{*} ligand (U1–Ct = 2.592 Å) bound to a uranium pinacolate supported by a ^{Mes}PDI^{Me} ligand (Figure 5, right; Table 2). The formerly aldehydic protons on the pinacolate ligand were also refined. The molecular structure shows the pinacolate ligand adopts a *meso* conformation with U–O distances (2.151(3) and 2.133(3) Å) similar to those in **5-Cp^P** and U(O₂C₂Ph₄)₂(THF)₂, supporting the hypothesis that steric bulk precludes formation of the benzophenone derivative. Similar to the case of **5-Cp^P**, the uranium is situated 1.032 Å above the plane of the ^{Mes}PDI^{Me} ligand.

Examination of the metrical parameters for ^{Mes}PDI^{Me} in **5-Cp^{*}** indicates a potentially differing electronic structure than for **5-Cp^P**. The N1–C2 and N3–C8 distances of 1.315(6) and 1.311(6) Å are similar to free ^{Mes}PDI^{Me}, supporting their double bond character, while the adjacent C–C distances of 1.441(6) (C2–C3) and 1.437(6) Å (C7–C8) show only a slight deviation from the free ^{Mes}PDI^{Me}, indicating little, if any, reduction. However, ligand reduction is most clear in the pyridine ring, where the C3–C4 (1.473(6) Å) and C6–C7 (1.479(6) Å) distances have been significantly elongated to the degree of C–C single bonds, while C4–C5 (1.397(7)) and C5–C6 (1.419(7)) possess multiple bond character. These parameters are in contrast to those noted for **5-Cp^P**, where the bond distances within the pyridine ring are similar to an aromatic system. A consequence of the unusual electronic structure of ^{Mes}PDI^{Me} observed for **5-Cp^{*}** is that the uranium–nitrogen distances show three dative linkages spanning 2.523(4)–2.568(4) Å. Thus, the metrical parameters suggest that a charge separated radical anion resonance form of the [^{Mes}PDI^{Me}][–] ligand is the dominant form in **5-Cp^{*}** (Figure 4, right; Table 2). As in the case of **5-Cp^P**, the trianionic ^{Mes}PDI^{Me} ligand in **3-Cp^{*}** is the source of the reducing equivalents for benzaldehyde activation to form **5-Cp^{*}**, which maintains a uranium(IV) center.

Examination of the electronic absorption spectra of **1-Cp^{*}**, **1-Cp^P**, **5-Cp^P**, and **5-Cp^{*}** further highlights electronic structure differences. Complexes **1-Cp^{*}**, **1-Cp^P**, and **5-Cp^P** are all dark brown and display similar, ill-defined, relatively strong transitions (ε = 200–888 M^{–1} cm^{–1}) throughout the near-infrared region (Figure 6). These transitions are thought to result from intramolecular electron transfer (IET) between the [^{Mes}PDI^{Me}][–] radical and the uranium(IV) center. Bands of similar energy and intensity in the near-infrared region have been observed in Me₃Fc-PTM, which is an octamethylferrocene linked through a conjugated vinylene bridge to a perchlorotriphenylmethyl (PTM) radical. In this case, bands assigned to the IET result from an electron transfer from the Me₃Fc (donor) to the PTM (acceptor). These bands in the near-infrared region are absent for the valence tautomeric species, Me₃Fc⁺–PTM[–].⁶¹ Instead, this zwitterionic form displays a diagnostic absorbance at 530 nm (ε ~ 11 000 M^{–1} cm^{–1}) assigned as the PTM anion charge transfer.⁶² The intense near-infrared bands observed for **1-Cp^{*}**, **1-Cp^P**, and **5-Cp^P** are in sharp contrast to **5-Cp^{*}**, which displays a typical U(IV)

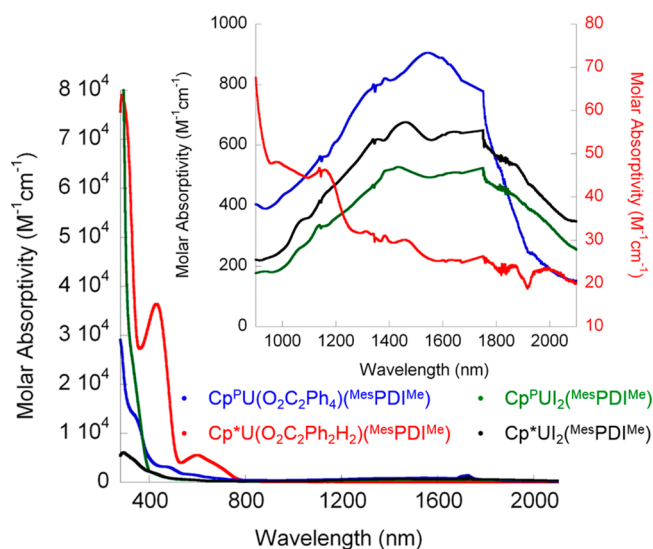


Figure 6. Electronic absorption spectra of complexes **1-Cp***, **1-Cp^P**, **5-Cp^P**, and **5-Cp*** recorded in THF at 25 °C. Solvent overtones between 1700 and 1800 nm have been removed for clarity.

absorbance spectrum with sharp, weakly intense ($\epsilon = 20\text{--}50 \text{ M}^{-1} \text{ cm}^{-1}$) transitions in the near-infrared region. The lack of the IET band supports that **5-Cp*** can be thought of as a zwitterionic complex. In addition to the differences in the near-IR region, bright green **5-Cp*** also contains two dominant features in the visible region assigned to the charge transfer of the pyridine anion ($\epsilon = 36\,430 \text{ M}^{-1} \text{ cm}^{-1}$, 431 nm) and to the color producing band ($5560 \text{ M}^{-1} \text{ cm}^{-1}$, 602 nm), the latter of which is analogous to that observed for green **4-Cp^P**.

The variation of the sterics and electronics of the cyclopentadienyl ligands is highlighted in the reactivity of **3-Cp^P** and **3-Cp***, as these rings ultimately determine substrate preference and electronic structures of the final products, **5-Cp*** and **5-Cp^P**. In the case of the **Cp^P** ligand, ketones can be reduced and coupled since the $-\text{Me}_2\text{Ph}$ substituent can rotate away from the uranium center, which serves to relieve the steric pressure. For the larger **Cp***, only activation of aldehydes is possible, since substrates are small enough to approach the uranium center. The dichotomy in the electronic structures of **5-Cp^P** and **5-Cp*** can be correlated to the electron donating ability of the cyclopentadienyl ring (Scheme 2). In the case of **Cp^P**, the pinacolite product features an anionic $\text{U}-\text{N}_{\text{pyr}}$ bond, forcing a $[\text{MesPDI}^{\text{Me}}]^{-1}$ radical. This occurs because the electron donating effect of the methyl groups is mediated by the withdrawing effect of the adjacent phenyl group on the **Cp** ligand. In contrast, the five alkyl substituents of **Cp*** create a highly electron donating ligand, such that the anionic charge of the $\text{U}-\text{N}_{\text{pyr}}$ bond is pushed onto the pyridine(diimine) ligand, converting it to a dative bond. This generates the zwitterionic

resonance form that is confirmed by the electronic absorption spectrum.

CONCLUSIONS

In conclusion, a series of reduced pyridine(diimine) uranium(IV) species with either the **Cp*** or **Cp^P** framework have been generated from uranium(III) starting materials. The entries in the series differ in the extent of pyridine(diimine) ligand reduction, which was made possible by treatment with potassium graphite. While analogous members of each series appear to be quite similar in their electronics and metrical parameters, the reactivity of the trianionic $[\text{MesPDI}^{\text{Me}}]^{3-}$ compounds with carbonylated substrates differs. With the sterically smaller **Cp^P** derivative, a new pinacolite compound is formed by benzophenone coupling, whereas reactivity with aldehydes results in decomposition. For the larger **Cp*** derivative, benzophenone is too bulky to react, but analogous coupling chemistry is possible with benzaldehyde. In the latter case, an unusual electronic structure for $[\text{MesPDI}^{\text{Me}}]^{-}$ is noted and formulated based on the metrical parameters.

The findings presented here highlight the ability of the pyridine(diimine) ligand to exist in multiple oxidation states, which in turn maintains the +4 valency of the uranium center. The trianionic ligands serve as electron sources to reduce C–O bonds and are oxidized over the course of the reactions. The redox-active $\text{MesPDI}^{\text{Me}}$ ligand facilitates multielectron chemistry at uranium, while investigating the effect of steric variation of the cyclopentadienyl ligand in the coordination sphere. Additionally, changing the electron donation ability of the cyclopentadienyl substituent dictates the electronic structure of the pyridine(diimine) ligand in the products. Ongoing studies are currently focused on the reactivity of this family of reduced uranium(IV) compounds for small molecule activation.

ASSOCIATED CONTENT

Supporting Information

¹H NMR spectra and crystallographic details. This material is available free of charge via the Internet at <http://pubs.acs.org>

AUTHOR INFORMATION

Corresponding Author

*E-mail: sbart@purdue.edu.

Author Contributions

The manuscript was written through contributions of all authors. All authors have given approval to the final version of the manuscript.

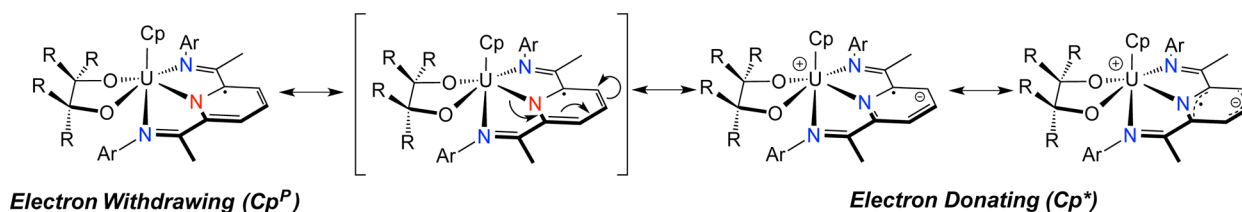
Notes

The authors declare no competing financial interest.

ACKNOWLEDGMENTS

The authors acknowledge partial support from the Donors of the American Chemical Society Petroleum Research Fund, as

Scheme 2. Influence of **Cp** Ligand on Pinacolite Product Electronic Structure



well as from the Division of Chemical Sciences, Geosciences, and Biosciences, Office of Basic Energy Sciences of the U.S. Department of Energy through Grant DE-AC02-12ER16328 (SCB). The National Science Foundation (NSF-CHE-1058889, grant to MPS) is also acknowledged. SCB is a Cottrell Scholar funded by the Research Corporation.

REFERENCES

- (1) Reynolds, L. T.; Wilkinson, G. *J. Inorg. Nucl. Chem.* **1956**, *2*, 246.
- (2) Kanellakopulos, B.; Fischer, E. O.; Dornberger, E.; Baumgartner, F. *J. Organomet. Chem.* **1970**, *24*, 507.
- (3) Fischer, E. O.; Hristidu, Y. Z. *Naturforsch.* **1962**, *17b*, 275.
- (4) Manriquez, J. M.; Fagan, P. J.; Marks, T. J. *J. Am. Chem. Soc.* **1978**, *100*, 3939.
- (5) Duval, P. B.; Burns, C. J.; Clark, D. L.; Morris, D. E.; Scott, B. L.; Thompson, J. D.; Werkema, E. L.; Jia, L.; Andersen, R. A. *Angew. Chem., Int. Ed.* **2001**, *40*, 3357.
- (6) Graves, C. R.; Scott, B. L.; Morris, D. E.; Kiplinger, J. L. *Organometallics* **2008**, *27*, 3335.
- (7) Pool, J. A.; Scott, B. L.; Kiplinger, J. L. *J. Am. Chem. Soc.* **2005**, *127*, 1338.
- (8) Kiplinger, J. L.; John, K. D.; Morris, D. E.; Scott, B. L.; Burns, C. J. *Organometallics* **2002**, *21*, 4306.
- (9) Marks, T. J.; Seyam, A. M.; Kolb, J. R. *J. Am. Chem. Soc.* **1973**, *95*, 5529.
- (10) Boisson, C.; Berthet, J.-C.; Lance, M.; Nierlich, M.; Vigner, J.; Ephritikhine, M. *J. Chem. Soc., Chem. Commun.* **1995**, 543.
- (11) Evans, W. J.; Nyce, G. W.; Forrestal, K. J.; Ziller, J. W. *Organometallics* **2002**, *21*, 1050.
- (12) Evans, W. J.; Nyce, G. W.; Johnston, M. A.; Ziller, J. W. *J. Am. Chem. Soc.* **2000**, *122*, 12019.
- (13) Manriquez, J. M.; Fagan, P. J.; Marks, T. J.; Vollmer, S. H.; Day, C. S.; Day, V. W. *J. Am. Chem. Soc.* **1979**, *101*, 5075.
- (14) Fagan, P. J.; Manriquez, J. M.; Marks, T. J.; Day, C. S.; Vollmer, S. H.; Day, V. W. *Organometallics* **1982**, *1*, 170.
- (15) Graves, C. R.; Yang, P.; Kozimor, S. A.; Vaughn, A. E.; Clark, D. L.; Conradson, S. D.; Schelter, E. J.; Scott, B. L.; Thompson, J. D.; Hay, P. J.; Morris, D. E.; Kiplinger, J. L. *J. Am. Chem. Soc.* **2008**, *130*, 5272.
- (16) Fagan, P. J.; Manriquez, J. M.; Maatta, E. A.; Seyam, A. M.; Marks, T. J. *J. Am. Chem. Soc.* **1981**, *103*, 6650.
- (17) Kiplinger, J. L.; Morris, D. E.; Scott, B. L.; Burns, C. J. *Organometallics* **2002**, *21*, 3073.
- (18) Evans, W. J.; Traina, C. A.; Ziller, J. W. *J. Am. Chem. Soc.* **2009**, *131*, 17473.
- (19) Cladis, D. P.; Kiernicki, J. J.; Fanwick, P. E.; Bart, S. C. *Chem. Commun.* **2013**, *49*, 4169.
- (20) Pangborn, A. B.; Giardello, M. A.; Grubbs, R. H.; Rosen, R. K.; Timmers, F. J. *Organometallics* **1996**, *15*, 1518.
- (21) Chakraborty, S.; Chattopadhyay, J.; Guo, W.; Billups, W. E. *Angew. Chem., Int. Ed.* **2007**, *46*, 4486.
- (22) Avens, L. R.; Burns, C. J.; Butcher, R. J.; Clark, D. L.; Gordon, J. C.; Schake, A. R.; Scott, B. L.; Watkin, J. G.; Zwick, B. D. *Organometallics* **2000**, *19*, 451.
- (23) Alt, H. G.; Reb, A.; Kundu, K. *J. Organomet. Chem.* **2001**, *628*, 211.
- (24) Monreal, M. J.; Thomson, R. K.; Cantat, T.; Travia, N. E.; Scott, B. L.; Kiplinger, J. L. *Organometallics* **2011**, *30*, 2031.
- (25) Britovsek, G. J. P.; Bruce, M.; Gibson, V. C.; Kimberley, B. S.; Maddox, P. J.; Mastroianni, S.; McTavish, S. J.; Redshaw, C.; Solan, G. A.; Stroemberg, S.; White, A. J. P.; Williams, D. J. *J. Am. Chem. Soc.* **1999**, *121*, 8728.
- (26) Sheldrick, G. M. *Acta Crystallogr.* **2008**, *A64*, 112.
- (27) Beurskens, P. T.; Beurskens, G.; de Gelder, R.; Garcia-Granda, S.; Gould, R. O.; Smits, J. M. M. *DIRDIF2008 Program System*; Crystallography Laboratory, University of Nijmegen: The Netherlands, 2008.
- (28) Bain, G. A.; Berry, J. F. *J. Chem. Educ.* **2008**, *85*, 532.
- (29) Maynadie, J.; Berthet, J.-C.; Thuery, P.; Ephritikhine, M. *Organometallics* **2006**, *25*, 5603.
- (30) Knijnenburg, Q.; Gambarotta, S.; Budzelaar, P. H. M. *Dalton Trans.* **2006**, 5442.
- (31) Bart, S. C.; Chlopek, K.; Bill, E.; Bouwkamp, M. W.; Lobkovsky, E.; Neese, F.; Wieghardt, K.; Chirik, P. J. *J. Am. Chem. Soc.* **2006**, *128*, 13901.
- (32) De Bruin, B.; Bill, E.; Bothe, E.; Weyhermüller, T.; Wieghardt, K. *Inorg. Chem.* **2000**, *39*, 2936.
- (33) Monreal, M. J.; Diaconescu, P. L. *Organometallics* **2008**, *27*, 1702.
- (34) Bart, S. C.; Anthon, C.; Heinemann, F. W.; Bill, E.; Edelstein, N. M.; Meyer, K. *J. Am. Chem. Soc.* **2008**, *130*, 12536.
- (35) Stewart, J. L.; Andersen, R. A. *Polyhedron* **1998**, *17*, 953.
- (36) Kraft, S. J.; Williams, U. J.; Daly, S. R.; Schelter, E. J.; Kozimor, S. A.; Boland, K. S.; Kikkawa, J. M.; Forrest, W. P.; Christensen, C. N.; Schwarz, D. E.; Fanwick, P. E.; Clark, D. L.; Conradson, S. D.; Bart, S. C. *Inorg. Chem.* **2011**, *50*, 9838.
- (37) Evans, W. J.; Forrestal, K. J.; Ziller, J. W. *Angew. Chem., Int. Ed. Engl.* **1997**, *36*, 774.
- (38) Brennan, J. G.; Stults, S. D.; Andersen, R. A.; Zalkin, A. *Organometallics* **1988**, *7*, 1329.
- (39) Del Mar Conejo, M.; Parry, J. S.; Carmona, E.; Schultz, M.; Brenmann, J. G.; Beshouri, S. M.; Andersen, R. A.; Rogers, R. D.; Coles, S.; Hursthouse, M. *Chem.—Eur. J.* **1999**, *5*, 3000.
- (40) Avens, L. R.; Bott, S. G.; Clark, D. L.; Sattelberger, A. P.; Watkin, J. G.; Zwick, B. D. *Inorg. Chem.* **1994**, *33*, 2248.
- (41) Antunes, M. A.; Pereira, L. C. J.; Santos, I. C.; Mazzanti, M.; Marcalo, J.; Almeida, M. *Inorg. Chem.* **2011**, *50*, 9915.
- (42) Rinehart, J. D.; Long, J. R. *J. Am. Chem. Soc.* **2009**, *131*, 12558.
- (43) Rinehart, J. D.; Meihaus, K. R.; Long, J. R. *J. Am. Chem. Soc.* **2010**, *132*, 7572.
- (44) Coutinho, J. T.; Antunes, M. A.; Pereira, L. C. J.; Bolvin, H.; Marcalo, J.; Mazzanti, M.; Almeida, M. *Dalton Trans.* **2012**, *41*, 13568.
- (45) Newell, B. S.; Schwaab, T. C.; Shores, M. P. *Inorg. Chem.* **2011**, *50*, 12108.
- (46) Seaman, L. A.; Pedrick, E. A.; Tsuchiya, T.; Wu, G.; Jakubikova, E.; Hayton, T. W. *Angew. Chem., Int. Ed.* **2013**, *52*, 10589.
- (47) Bouwkamp, M. W.; Bart, S. C.; Hawrelak, E. J.; Trovitch, R. J.; Lobkovsky, E.; Chirik, P. J. *Chem. Commun.* **2005**, 3406.
- (48) Archer, A. M.; Bouwkamp, M. W.; Cortez, M.-P.; Lobkovsky, E.; Chirik, P. J. *Organometallics* **2006**, *25*, 4269.
- (49) Qian, Y.; Huang, J.; Yang, J.; S.C. Chan, A.; Chen, W.; Chen, X.; Guisheng, L.; Jin, X.; Yang, Q. *J. Organomet. Chem.* **1997**, *547*, 263.
- (50) H. Doerrer, L.; L. H. Green, M.; Hau; Sam. *J. Chem. Soc., Dalton Trans.* **1999**, 2111.
- (51) Sassmannshausen, J.; Powell, A. K.; Anson, C. E.; Wocadlo, S.; Bochmann, M. *J. Organomet. Chem.* **1999**, *592*, 84.
- (52) Centore, R.; Csok, Z.; Tuzi, A. *Acta Crystallogr., Sect. C: Cryst. Struct. Commun.* **2004**, *60*, m625.
- (53) Deng, M.; Yao, Y.; Shen, Q.; Zhang, Y.; Lang, J.; Zhou, Y. *J. Organomet. Chem.* **2003**, *681*, 174.
- (54) Otten, E.; Batinas, A. A.; Meetsma, A.; Hessen, B. *J. Am. Chem. Soc.* **2009**, *131*, 5298.
- (55) Mohammad, A.; Cladis, D. P.; Forrest, W. P.; Fanwick, P. E.; Bart, S. C. *Chem. Commun.* **2012**, *48*, 1671.
- (56) Villiers, C.; Adam, R.; Lance, M.; Nierlich, M.; Vigner, J.; Ephritikhine, M. *J. Chem. Soc., Chem. Commun.* **1991**, 1144.
- (57) Summerscales, O. T.; Cloke, F. G. N.; Hitchcock, P. B.; Green, J. C.; Hazari, N. *J. Am. Chem. Soc.* **2006**, *128*, 9602.
- (58) Frey, A. S. P.; Cloke, F. G. N.; Coles, M. P.; Hitchcock, P. B. *Chem.—Eur. J.* **2010**, *16*, 9446.
- (59) Lam, O. P.; Anthon, C.; Heinemann, F. W.; O'Connor, J. M.; Meyer, K. *J. Am. Chem. Soc.* **2008**, *130*, 6567.
- (60) Maury, O.; Villiers, C.; Ephritikhine, M. *Tetrahedron Lett.* **1997**, *38*, 6591.
- (61) Guasch, J.; Grisanti, L.; Jung, S.; Morales, D.; D'Avino, G.; Souto, M.; Fontrodona, X.; Painelli, A.; Renz, F.; Ratera, I.; Veciana, J. *Chem. Mater.* **2013**, *25*, 808.

(62) Ratera, I.; Sporer, C.; Ruiz-Molina, D.; Ventosa, N.; Baggerman, J.; Brouwer, A. M.; Rovira, C.; Veciana, J. *J. Am. Chem. Soc.* **2007**, *129*, 6117.